WILEY

Analysis of the escape in systems with four exit channels

Juan F. Navarro (iD) | **Ibrahim Belgharbi** | **María del Carmen Martínez-Belda**

Department of Applied Mathematics, University of Alicante, Alicante, Spain

Correspondence
Juan F. Navarro, Carretera San Vicente del Raspeig s/n, 03690 Alicante.
Email: jf.navarro@ua.es

Communicated by: J. Vigo-Aguiar

In this paper, we have performed a numerical investigation of the escape of a particle from two different dynamical systems with the same number of exit channels. We have chosen specific values of the parameters of the systems so that the openings of the potential well in both systems are approximately of the same size. We have found that, in the galactic system, the distribution of the times of escape follows a sequential pattern that has never been detected before. Moreover, we have proved that this pattern is directly related to the geometry of the stable manifolds to the Lyapunov orbits located at the openings of the potential. Finally, we have shown that the different nature of the two systems affects the way the escape occurs, due to the difference in the geometry of the manifolds to the Lyapunov orbits in both systems.

1 | INTRODUCTION

The analysis of the escape of a test particle from a dynamical system is an active field of research to which many scientists are contributing nowadays.[1-19] The mechanism that explains how the escape from a system takes place is well known: The limiting curve of the basins of escape in a proper surface of section is determined by projecting the stable manifolds to the unstable periodic orbits that are located at the openings of the curves of zero velocity of the system on this surface. However, it is necessary to calculate these limiting curves in each specific system in order to unveil the properties of the escape. There is also another possible approach to the problem, consisting of calculating numerically the basins of escape through the integration of a mesh of initial conditions taken on the surface of section, and considering a maximum integration time, so that if the particle has not escaped at that time, it is considered to be trapped forever.

We also can find some comparative analysis that try to extract universal properties of the escape in different types of systems. For instance, Siopis et al[17] performed a numerical study of the escape in three time-independent potentials possessing different types of symmetries, finding that there is a rather abrupt transition in the behavior of the late-time probability of escape, when the value of a transition parameter exceeds a critical value. For any value of the transition parameter larger than the critical value, the probability of escape initially converges to a nearly time-independent value, exhibiting a simple scaling that may be universal.

The aim of this work is to analyze if there is any property of the escape depending exclusively on the number of openings of the system. To that end, we start exploring the escape in two systems of different nature but with the same number of

exit channels. We have taken specific values of the parameters of the systems such that the openings of the potential well in both systems are approximately of the same size.

1. On the one hand, we deal with the escape in the N-body ring problem, when $N = 4$ and the potential well has four openings.
2. On the other hand, we study a simple local galactic potential describing the motion near the center of a elliptical galaxy.

We show how the number of escaping orbits tends to zero as the time of escape becomes larger in both systems, despite of the fact that, for short times of escape, the distribution of the number of escaping orbits is significantly different in both systems. In the four-body ring problem, this distribution appears to be approximately uniform and slowly decreasing with time, for times of escape from 0 to 40, and considering intervals of time of unit size. However, in the galactic system, the fast escape follows a sequential pattern. This different behavior is due to the shape of the geometric curves obtained when the stable manifolds to the Lyapunov orbits located at the openings of the curves of zero velocity are projected on the surfaces of section in both systems. In some sense, we can state that these projections have an ordered structure in the galactic system and has a more intertwined architecture in the N-body ring problem.

2 | SYSTEMS WITH FOUR EXIT CHANNELS

In this section, we present the two systems we are going to analyze. For both of them, there exists a value of the energy such that if the energy is larger than this critical value, the potential well opens up at four places in the configuration space. We have selected the value of the energy in both systems to obtain openings of approximately the same size. Each of the openings of the curves of zero velocity is bridged by a highly unstable periodic orbit, called Lyapunov orbit. The main property of these orbits is that if an orbit crosses one of them outwards, then this orbit escapes from the system, as always moves outwards.

2.1 | The four-body ring problem

The four-body ring problem describes the motion of a particle S of negligible mass, moving under the gravitational influence of five bodies (called primaries) laid out in a planar circular configuration. The main body, of mass m_0, is located at the center of mass of the system. The other four bodies, all of them with the same mass m, are situated at the vertexes of a regular polygon that rotates on its own plane around the center of mass with a uniform angular velocity.[14,15,20]

The dimensionless equations of motion describing the motion in a plane of a test particle under the gravitational influence of this system are given by

$$\ddot{x} - 2\dot{y} = \frac{\partial U_{4BRP}}{\partial x}, \quad \ddot{y} + 2\dot{x} = \frac{\partial U_{4BRP}}{\partial y}, \tag{1}$$

where $U_{4BRP}(x, y)$ is the potential given by

$$U_{4BRP}(x, y) = \frac{1}{2}(x^2 + y^2) + \frac{1}{\Delta}\left(\frac{\beta}{r_0} + \sum_{\nu=1}^{4}\frac{1}{r_\nu}\right),$$

$\beta = m_0/m$ is the relation between the central mass and the mass of one of the peripherals, $r_0 = \sqrt{x^2 + y^2}$ is the distance of the test particle to the central body, and

$$r_\nu = \sqrt{(x - x_\nu^*)^2 + (y - y_\nu^*)^2},$$

for $\nu = 1, 2, 3, 4$, are the distances of the test particle from the peripheral primaries. The quantities x_ν^* and y_ν^* are the coordinates of the peripheral bodies,

$$x_\nu^* = \frac{1}{2\sin\theta}\cos(2(\nu - 1)\theta), \quad y_\nu^* = \frac{1}{2\sin\theta}\sin(2(\nu - 1)\theta),$$

and Δ is given by

$$\Delta = M(\Lambda + \beta M^2),$$

where

$$\Lambda = \sum_{\nu=2}^{4}\frac{\sin^2\theta\cos((3 - \nu)\theta)}{\sin^2((5 - \nu)\theta)} = \sum_{\nu=2}^{4}\frac{\sin^2\theta}{\sin((\nu - 1)\theta)},$$

and

$$M = \sqrt{2(1 - \cos\psi)} = 2\sin\theta.$$

In these formulas, ψ is the angle between the central and two successive peripheral primaries, and $\theta = \psi/2 = \pi/4$.

In this formulation, we have considered a reference frame rotating at a constant angular velocity equal to the unit, such that its origin corresponds to the center of mass of the main body, and taking the x axis on the line joining the main body with one of the primaries on the ring.

This system has a Jacobi-type integral of motion, which is given by

$$C = 2U_{4BRP}(x, y) - (\dot{x}^2 + \dot{y}^2), \tag{2}$$

where C stands for the Jacobi constant.

The curves of zero velocity establish the limits of the motion of the test particle, and can be calculated through

$$C = 2U_{4BRP}(x, y) = x^2 + y^2 + \frac{2}{\Delta}\left(\frac{\beta}{r_0} + \sum_{\nu=1}^{N}\frac{1}{r_\nu}\right). \tag{3}$$

For a given value of β, there is a critical value C_e of the Jacobi constant such that, if the value of C is smaller than C_e, the curves of zero velocity are open and test particles may escape. In our experiments, we have taken $C = 2.74$. We show the curves of zero velocity of the system for this value of the Jacobi constant in the left panel of Figure 1.

2.2 | A guartic galactic potential

The second system we consider is a simple local galactic potential describing the motion near the center of an elliptical galaxy, given by

$$U_G(x, y) = \frac{1}{2}(\omega_1^2 x^2 + \omega_2^2 y^2) - \mu\left(\beta(x^4 + y^4) + 2\alpha x^2 y^2\right), \tag{4}$$

where ω_1, ω_2 are the unperturbed frequencies of oscillation along the x and y axes, respectively; $\mu > 0$ is the perturbation strength; and α and β are positive parameters.[7] Here, we analyze the case $\omega_1 = \omega_2 = 1$, that is, the $1:1$ resonance case. This galactic potential can only model the local motion of a star at short distances from the center of the galaxy. This is due to the fact that alternatively, the mass density grows in an outwardly direction from the center, a fact that is not usual in the observed galaxies. The Hamiltonian related to the potential (4) is given by

$$\mathcal{H} = \frac{1}{2}(\dot{x}^2 + \dot{y}^2) + \frac{1}{2}(x^2 + y^2) - \mu\left(\beta(x^4 + y^4) + 2\alpha x^2 y^2\right), \tag{5}$$
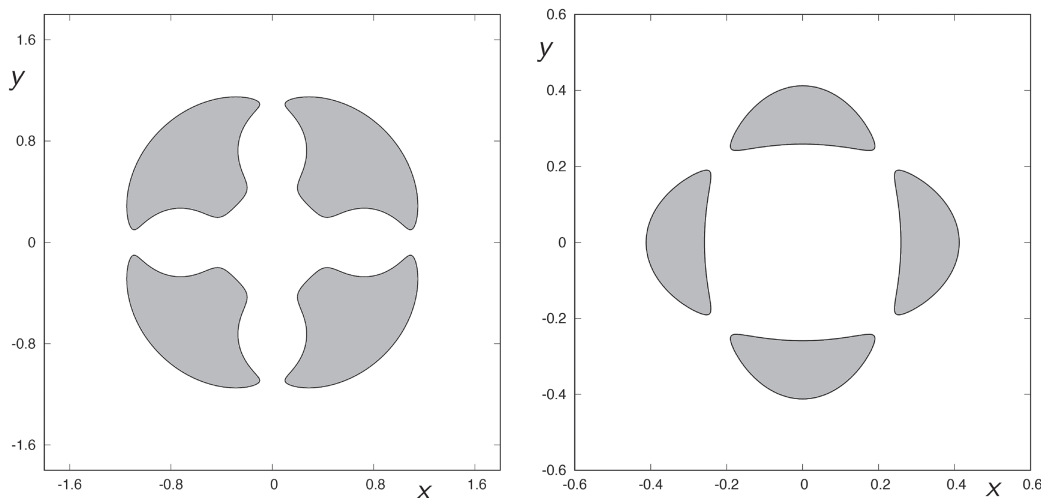
FIGURE 1 In the left panel, curves of zero velocity in the four-body ring problem, for $C = 2.74$ and $\beta = 2$. In the right panel, curves of zero velocity in the galactic problem, for $\mu = 2.64$, $\alpha = 1.2$, $\beta = 0.8$, and $h = 0.024$. The regions where the motion of the test particle is impossible to happen are colored in gray

and the curves of zero velocity are defined by the equation

$$2h = x^2 + y^2 - 2\mu\left(\beta(x^4 + y^4) + 2\alpha x^2 y^2\right),$$

where h is the energy of the system. In our analysis, we will choose the following values of the parameters of the system: $\mu = 2.64$, $\alpha = 1.2m$ and $\beta = 0.8$. For these values of the parameters, the critical value of the energy is $h_c = 0.0236742$. For each larger value of h, there is an unstable periodic orbit across the opening, bouncing back and forth between the two "walls" of the pass. In this paper, we have taken $h = 0.024$. The right panel of Figure 1 shows the curves of zero velocity for that value of the energy.

3 | ANALYSIS OF THE NUMERICAL RESULTS

In order to perform a numerical exploration of the escape from the systems described in Section 2, we take as surface of section the hyperplane $y = 0$, $\dot{y} > 0$. In this surface, we have defined a grid of 512×512 initial conditions equally spaced in the domain of the surface of section allowed by the value of the Jacobi constant in the four-body problem and
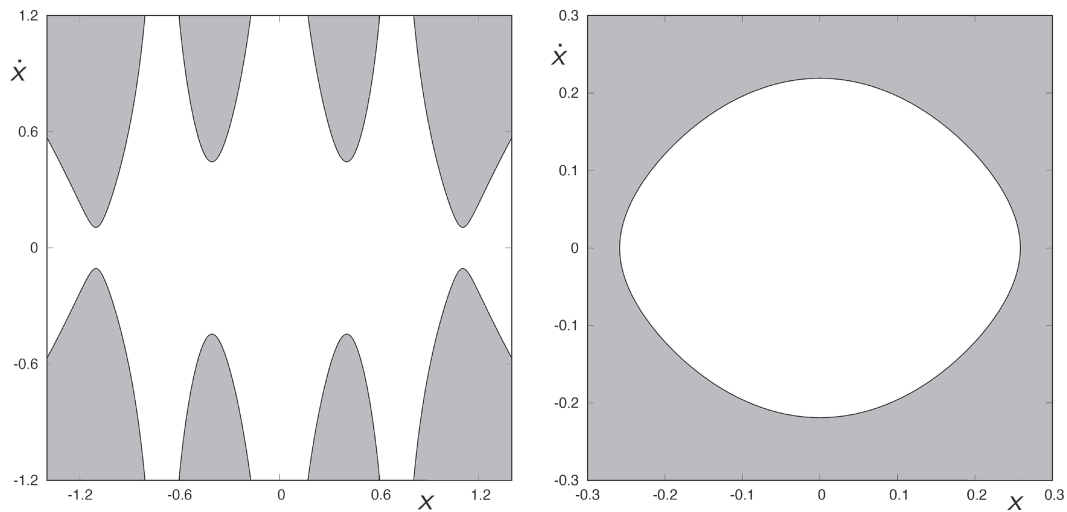

FIGURE 2 Regions D_{4BRP} (left panel) and D_G (right panel) of allowed initial conditions

TABLE 1 Number of orbits that escape from the system

t_1	t_2	$M_{e,4BRP}(t_1, t_2)$	$M_G(t_1, t_2)$
0	10	9,135	7,542
10	20	9,250	474
20	30	7,466	770
30	40	6,370	234
40	50	5,615	72
50	60	5,193	42
60	70	4,667	34
70	80	4,266	18
80	90	3,863	12
90	100	3,486	10
100	200	21,057	16
200	300	8,491	12
300	400	3,389	9
400	500	1,490	8
500	600	647	3
600	700	317	4
700	800	153	4
800	900	74	1
900	1,000	51	4
0	1,000	94,980	9,269

by the energy in the galactic system. The sets of initial conditions are taken in the $(x, \dot{x})$ space. If the values of the initial conditions $(x_0, \dot{x}_0)$ are given, subjected to $y_0 = 0$, then

1. In the four-body ring problem, $\dot{y}$ is calculated through

$$\dot{y} = +\sqrt{2U_{4BRP}(x_0, 0) - C - \dot{x}_0^2}.$$

2. In the galactic system, $\dot{y}$ is calculated through

$$\dot{y} = +\sqrt{2h - x_0^2 - \dot{x}_0^2 + 2\mu\beta x_0^4}.$$

Under these assumptions, for the four-body ring problem, the initial conditions are taken in the domain D_{4BRP} defined by

$$D_{4BRP} = \{(x_0, \dot{x}_0) \in \mathbb{R}^2 \ : \ 2U_{4BRP}(x_0, 0) - C - \dot{x}_0^2 \geq 0\}. \tag{6}$$

t_1	t_2	$R_{e,4BRP}(t_1, t_2)$	$R_{e,G}(t_1, t_2)$
0	10	0.0961781	0.81368
10	20	0.0973889	0.0511382
20	30	0.078606	0.0830726
30	40	0.0670668	0.0252454
40	50	0.0591177	0.00776783
50	60	0.0546747	0.00453123
60	70	0.0491367	0.00366814
70	80	0.0449147	0.00194196
80	90	0.0406717	0.00129464
90	100	0.0367025	0.00107887
100	200	0.2216993	0.0017262
200	300	0.0893978	0.00129464
300	400	0.0356812	0.000971
400	500	0.0156875	0.0008631
500	600	0.006812	0.00032366
600	700	0.0033375	0.000431546
700	800	0.0016109	0.000431546
800	900	0.0007791	0.000107892
900	1,000	0.0005369	0.000431546

TABLE 2 Relation between the orbits that escape in the interval $(t_1, t_2]$ and the total number of orbits that escape from the system before t_{max}
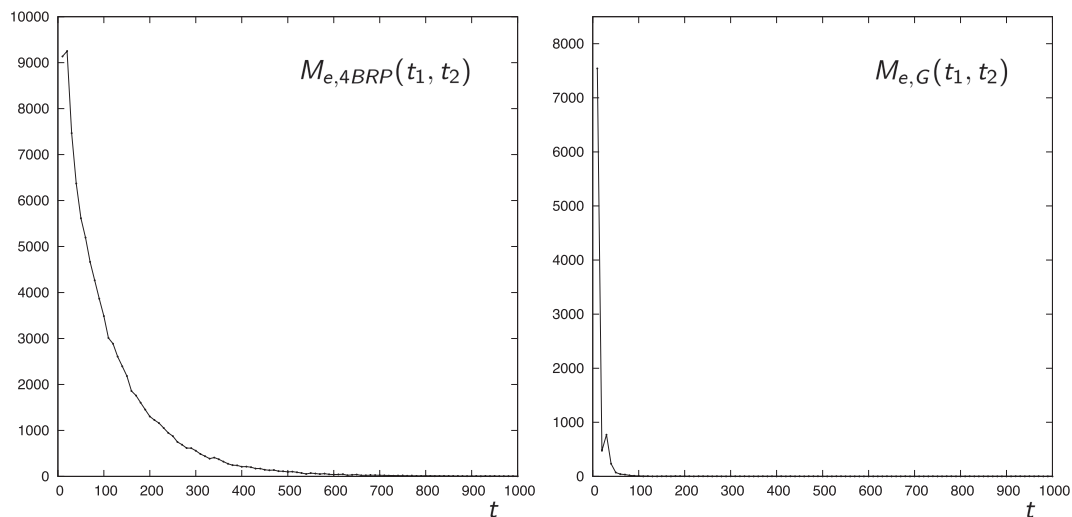
FIGURE 3 $M_{e,4BRP}(t_1, t_2)$ (left panel) and $M_{e,G}(t_1, t_2)$, considering $t_2 - t_1 = 10$
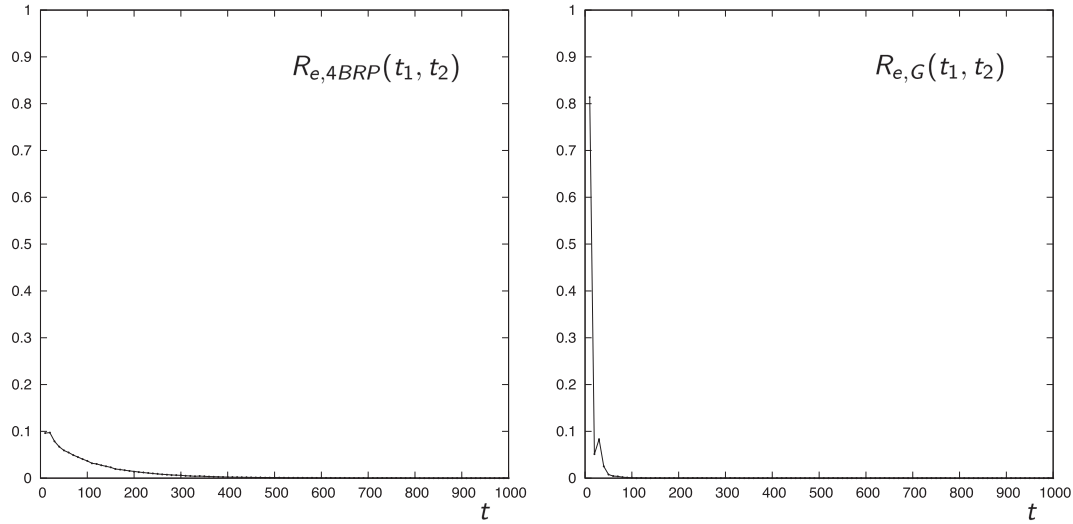
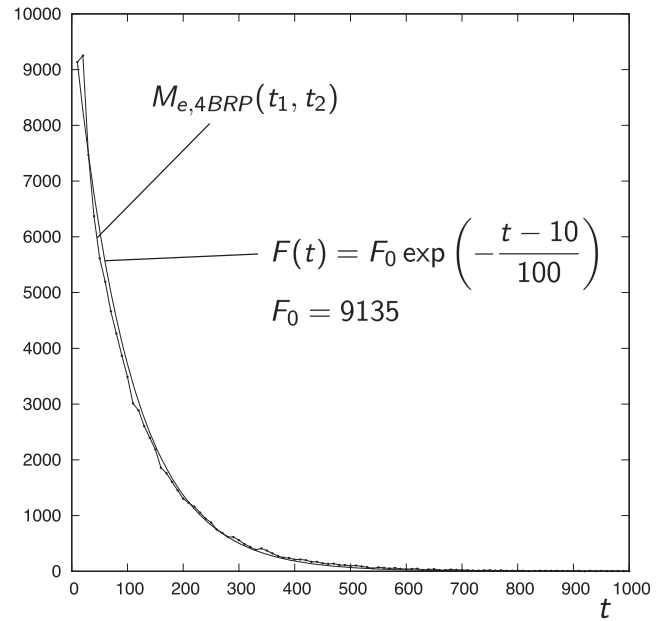**FIGURE 4** $R_{e,4BRP}(t_1, t_2)$ (left panel) and $R_{e,G}(t_1, t_2)$, considering $t_2 - t_1 = 10$

FIGURE 5 Joint representation of $M_{e,4BRP}(t_1, t_2)$ and $F(t) = F_0 \exp\left(-\frac{t-10}{100}\right)$, with $F_0 = 9135$

The initial conditions in the galactic system are taken in the domain D_G given by

$$D_G = \{(x_0, \dot{x}_0) \in \mathbb{R}^2 \ : \ 2h - x_0^2 - \dot{x}_0^2 + 2\mu\beta x_0^4 \geq 0\}. \tag{7}$$

In Figure 2, we depict these domains. The left panel of Figure 2 shows the region of allowed initial conditions in the phase $(x, \dot{x})$, for the four-body ring problem, and $\beta = 2$, $N = 4$ and $C = 2.74$. In the right panel of Figure 2, we depict the same region for the galactic system, for $h = 0.024$.

According to Navarro and Martínez-Belda,[14] in order to carry out an analysis of the distribution of the times of escape, we perform the numerical exploration considering a maximum time of integration of $t_{max} = 10^3$. When integrating one initial condition in the domain of possible initial conditions in the surface of section, we consider two scenarios:

1. The particle escapes from the system through one of the four openings, with a time of escape smaller than t_{max}.
2. The particle is trapped in the potential well if the particle has not left the potential well for a time of integration of t_{max}.

Let us define the following quantities: M_{4BRP} and M_G denote the total number of initial conditions in the grid inside D_{4BRP} and D_G, respectively. $M_{e,4BRP}(t_1, t_2)$ and $M_{e,G}(t_1, t_2)$ denote the number of orbits that leave the potential well with a time of escape in the interval $(t_1, t_2]$, in the four-body ring problem and the galactic system, respectively. E_{4BRP} and E_G denote the total number of orbits that escape from the system with a time of escape smaller than t_{max}, that is,

$$E_{4BRP} = M_{e,4BRP}(0, t_{max}), \quad E_G = M_{e,G}(0, t_{max}).$$

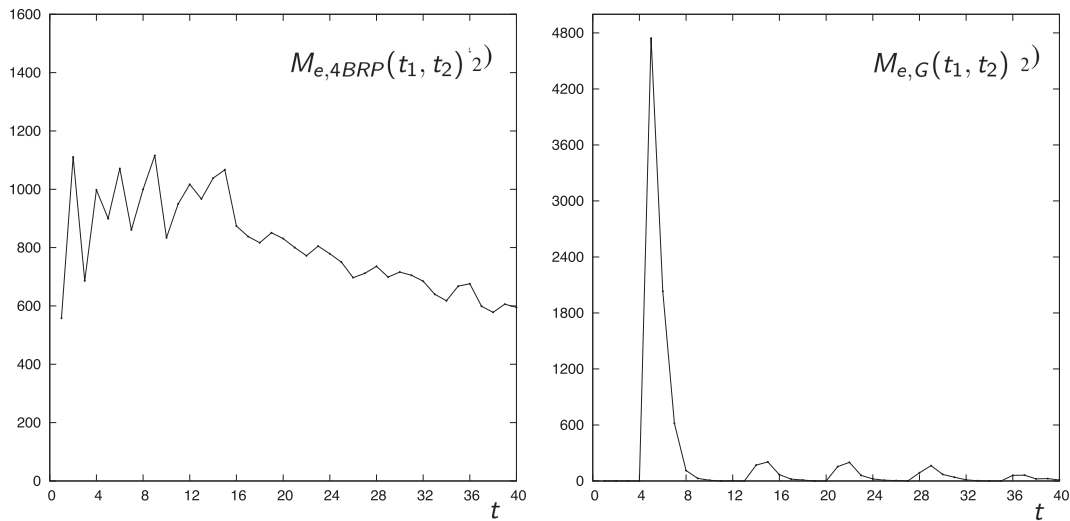We define the probability of escape between times t_1 and t_2 as

$$p_{e,4BRP}(t_1, t_2) = \frac{M_{e,4BRP}(t_1, t_2)}{M_{4BRP}}, \quad p_{e,G}(t_1, t_2) = \frac{M_{e,G}(t_1, t_2)}{M_G},$$

as well as the quantities

$$P_{4BRP}(t) = p_{e,4BRP}(0, t), \quad P_G(t) = p_{e,G}(0, t),$$

TABLE 3 Number of orbits that escape from the potential well during the first 40 units of time, considering $t_2 - t_1 = 1$

t_1	t_2	$M_{e,4BRP}(t_1, t_2)$	$M_{e,G}(t_1, t_2)$
0	1	558	0
1	2	1,111	0
2	3	686	0
3	4	998	0
4	5	900	4,744
5	6	1,071	2,032
6	7	861	618
7	8	1,000	112
8	9	1,116	28
9	10	834	8
10	11	950	0
11	12	1,017	2
12	13	967	0
13	14	1,038	170
14	15	1,067	204
15	16	874	68
16	17	838	20
17	18	817	10
18	19	851	0
19	20	831	0
20	21	800	154
21	22	772	200
22	23	805	60
23	24	779	22
24	25	750	8
25	26	697	4
26	27	712	0
27	28	736	88
28	29	699	164
29	30	716	70
30	31	705	40
31	32	685	12
32	33	640	2
33	34	618	0
34	35	668	0
35	36	676	60
36	37	599	62
37	38	578	22
38	39	606	26
39	40	595	10
0	40	32,221	9020

FIGURE 6 $M_{e,4BRP}(t_1, t_2)$ (left panel) and $M_{e,G}(t_1, t_2)$ (right panel), for times of escape smaller than 40 units of time, and considering $t_2 - t_1 = 1$

as the probability of escape before time t.

In this paper, we focus our interest in the relation between the orbits that escape in the interval $(t_1, t_2]$ and the total number of orbits that escape from the system before t_{max}, that is,

$$R_{e,4BRP}(t_1, t_2) = \frac{M_{e,4BRP}(t_1, t_2)}{E_{4BRP}}, \ R_{e,G}(t_1, t_2) = \frac{M_{e,G}(t_1, t_2)}{E_G}.$$

In the four-body ring problem, we have integrated 165,810 initial conditions, and 94,980 of them correspond to orbits that escape from the potential well. This means that 57.28% of the orbits escape. In the case of the galactic problem, we have integrated 195,460 initial conditions, and 9,269 of them correspond to orbits that leave the galactic system, that is, 4.74% of the orbits escape.

Table 1 shows the number of orbits that escape from the system with a time of escape between t_1 and t_2. For instance, 7,466 orbits escape in the four-body ring problem with a time of escape $t \in (20,30]$, and 770 orbits escape from the system in the galactic problem with a time of escape in the same interval. Table 2 shows the relation between the orbits that escape in the interval $(t_1, t_2]$ and the total number of orbits that escape from the system before t_{max}, that is, $R_{e,4BRP}(t_1, t_2)$ and $R_{e,G}(t_1, t_2)$. In Figures 3 and 4, we represent these results, considering intervals of time of 10 units of time, that is, with $t_2 - t_1 = 10$.

The left panel of Figure 3 and Table 1 show that, in the four-body ring problem, more than 18,000 orbits leave the potential well with a time of escape smaller than 20 units of time. The number of escaping orbits starts to decline about 1,000 orbits each 10 units of time until $t = 50$ units of time. The dependence of the number of escaping orbits on time is exponential in the four-body ring problem. In Figure 5, we represent $M_{e,4BRP}(t_1, t_2)$ together with the function

$$F(t) = F_0 \exp\left(-\frac{t-10}{100}\right),$$

with $F_0 = 9,135$. We observe that this function fits quite accurately the number of escaping orbits from the ring body potential. In the galactic system (right panel of Figure 3 and Table 1), we notice that 7,542 orbits escape from the system with a time of escape smaller than 10 units of time. Then, the number of escaping orbits descends drastically to 474 orbits that leave the potential well with times of escape in the interval (10,20]. In the interval (20,30], the number of escaping orbits increases to 770 orbits, and it decreases again to 234 orbits in the interval (30,40]. Then, it descends significantly, as we can observe in Table 1. We can conclude that there is a big difference in the number of escaping orbits and the probability of escape (Figure 4) between these two systems, despite of the fact that both systems have the same number of openings. This fact leads us to say that, in this case and for the values of the Jacobi constant and the energy we have considered, the number of openings is not relevant in the process of the escape in these two different systems.

In order to unveil how the escape from these systems happens during the first instants of time, we also show the number of orbits that escape from the potential well during the first 40 units of time, considering intervals of time $(t_1, t_2]$ with

$t_2 - t_1 = 1$, in Table 3 and Figure 6. Figure 6 makes clear that the fast escape from the system occurs in a very different way in the two systems we analyze. On the one hand, we observe that the number of orbits that escape from the potential well in the four-body ring problem remains above 600 for any of the unit intervals of the form $(t_1, t_2]$, with $t_2 - t_1 = 1$ and $t_1 = 0, 1, \ldots, 39$. As time increases, and goes beyond 20 units of time, we observe that a sustained and slight decrease in the number of orbits that leave the potential well per unit interval takes place. On the other hand, the galactic system behaves in a very different way. There are no escaping orbits with times of escape smaller than four units of time. Then, we find a main peak of escapes between $t = 4$ and $t = 8$. During this interval of time, more than 80% of the escapes from the system happens. For values of t larger than eight units of time, we find an almost periodic sequence in the structure in which the escape from the system takes place. We can observe that there are three small hills for the periods of times of escape (13,17), (20,24), and (27,31), respectively.

Thus, we can conclude that the escape occurs in a significantly different way in these two systems. Our results also suggest that the structure of the projections of the stable and unstable manifolds to the Lyapunov orbits located in the openings of the potential well on the surface of section $y = 0$ is completely different in those problems. In the four-body ring problem, the slight decrease in the number of orbits that leave the system indicates that the first intersections of the stable manifolds to the Lyapunov orbits with the surface of section are completely mixed. Moreover, the successive
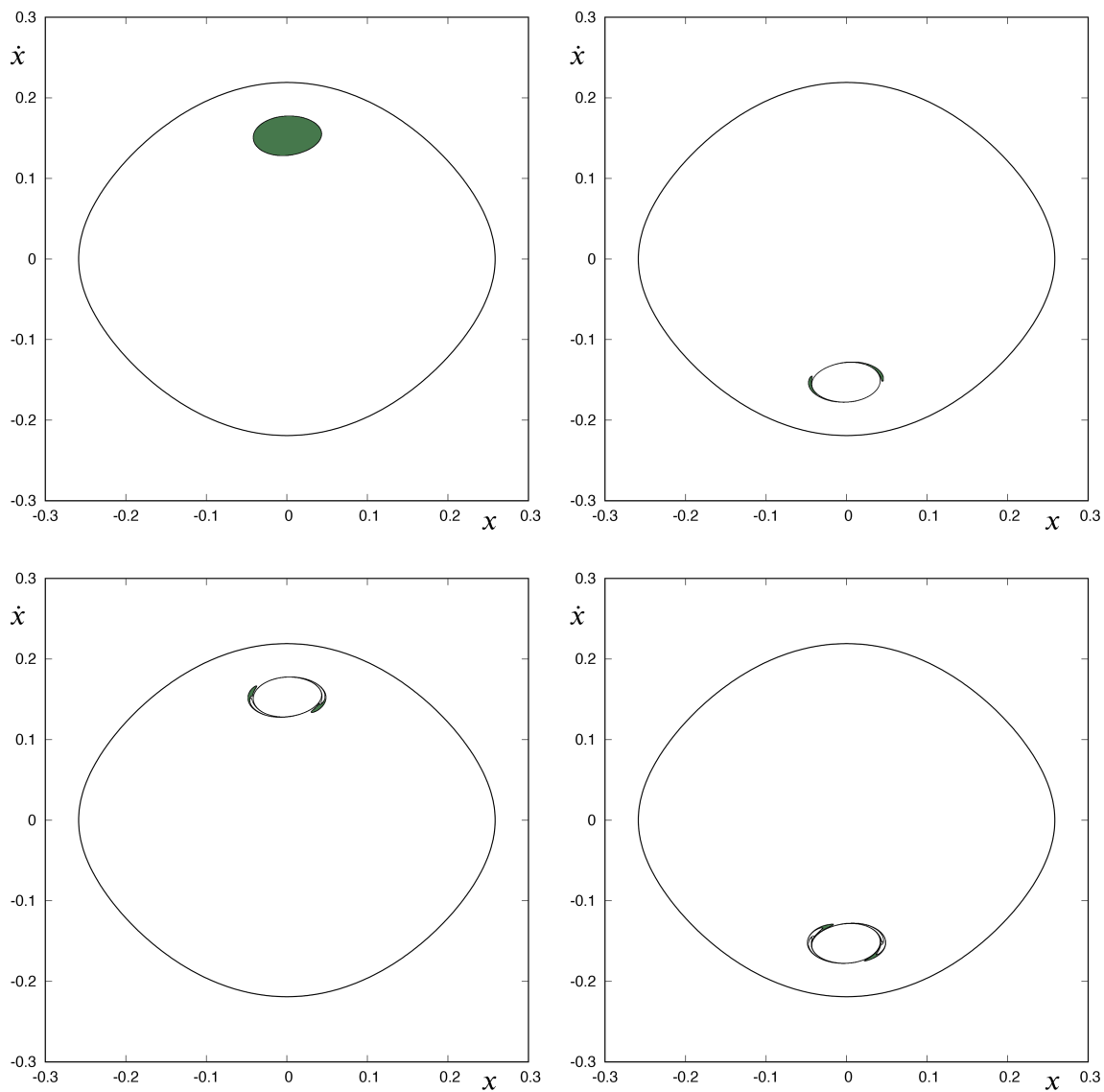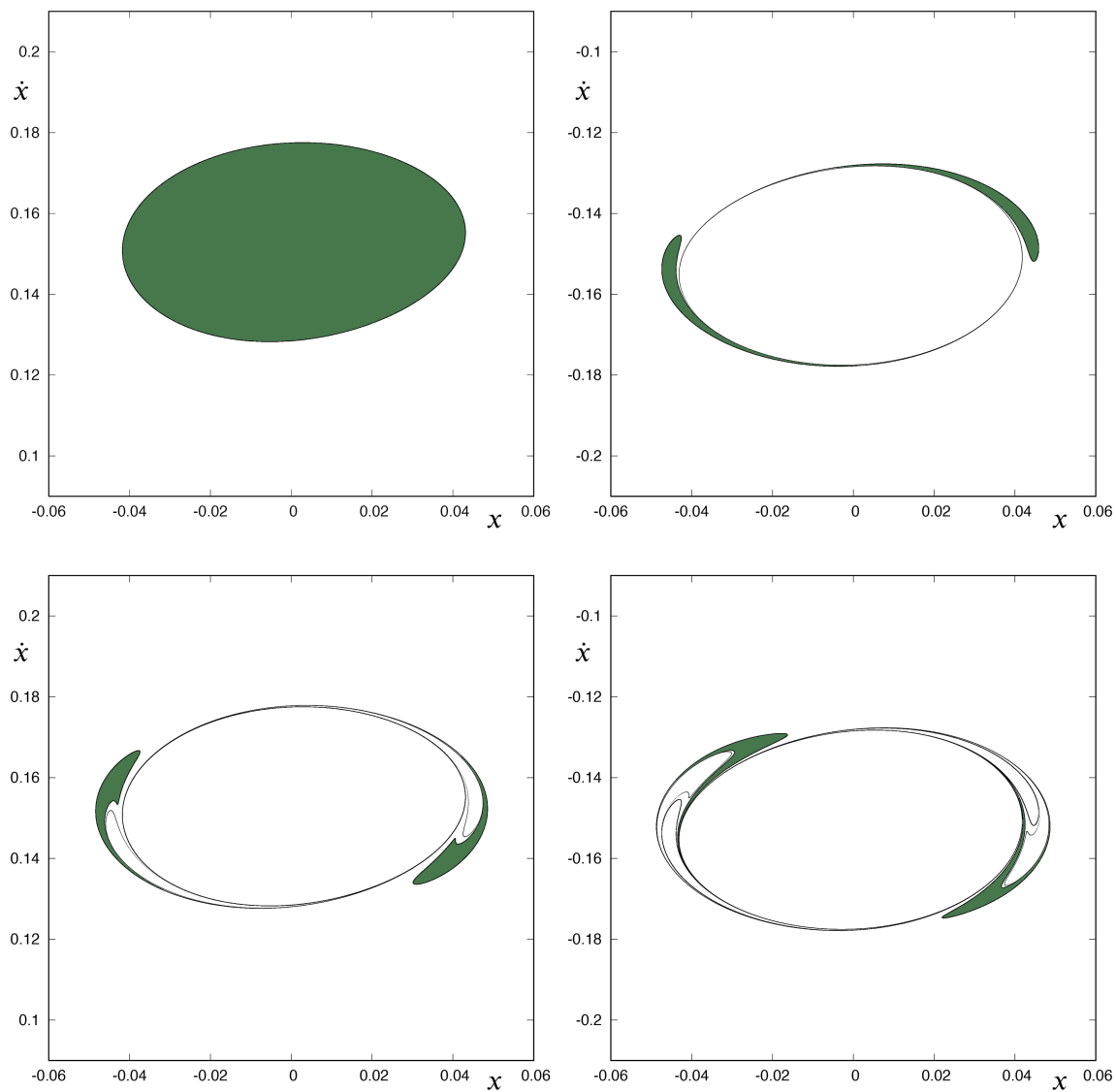

FIGURE 7 First (upper-left panel), second (upper-right panel), third (lower-left panel), and fourth (lower-right panel) intersections of the stable manifold to the first quadrant Lyapunov orbit with the surface of section $y = 0$. The region delimited by these curves has been colored in green [Colour figure can be viewed at wileyonlinelibrary.com]

intersections of the stable manifolds to the Lyapunov orbits with the surface of section we are considering occur at times that are almost equally distributed, from $t = 0$ to $t = 40$. This explains the slight decay in the number of escaping orbits.

The case of the galactic system is stranger, and we will analyze it in more detail. As we have commented, the fast escape from the galaxy takes place in a sequential fashion, step by step. Thus, we find a distribution of times of escape grouped around several centers: $t = 6$, $t = 14$, $t = 22$ and $t = 29$, as shown in the right panel of Figure 6. This means that the first crossings of the stable manifolds to each of the four Lyapunov orbits guarding the escape from the potential occur approximately at the same instants of time, and these instants of time are given by the sequence $t = 6, 14, 22, 29, \ldots$

In order to verify this assumption, we have integrated numerically and backward some 1,000,000 orbits belonging to the stable manifold to the first quadrant Lyapunov orbit (denoted by ϕ), until they cross the hyperplane $y = 0$, following the method described by Deprit and Henrard.[21] We have determined the first four crossings of this stable manifold with the surface of section. For each of the initial conditions, we have also computed the time at which the orbit crosses the surface of section for each of the four successive intersections with $y = 0$. Let us denote by $T_\nu \subset \mathbb{R}$, with $\nu = 1, 2, 3, 4$, to the intervals of time containing the set of instants of times at which the νth intersection of the orbits taken in the stable manifold to ϕ with the surface of section takes place. In Figures 7 and 8, we analyze the first (upper-left panel), second (upper-right panel), third (lower-left panel), and fourth (lower-right panel) intersections of the stable manifold to

FIGURE 8 Detail of the first (upper-left panel), second (upper-right panel), third (lower-left panel), and fourth (lower-right panel) intersections of the stable manifold to the first quadrant Lyapunov orbit with the surface of section $y = 0$. The region delimited by these curves has been colored in green [Colour figure can be viewed at wileyonlinelibrary.com]

the first quadrant Lyapunov orbit with the surface of section $y = 0$. We have colored in green the region limited by the curve defining each of the crossings. If we take an initial condition inside this green colored region, the corresponding orbit will leave the potential well. If the initial condition belongs to the region delimited by the νth intersection of the stable manifold with the surface of section, it will leave the galaxy after intersecting the surface of section $\nu - 1$ times. In Figure 8, we have depicted a zoom of these intersections to show the structures with more detail. The first intersection of the ingoing asymptotic trajectories to the periodic orbit ϕ with the surface of section is the closed curve shown in the upper-left panel of Figure 7. The intersection times belong to the interval $T_1 = (7.7, 8.6)$. All the initial conditions colored in green correspond to orbits that leave the potential well directly without intersecting the surface of section. The second intersection of the ingoing asymptotic trajectories to the periodic orbit ϕ, shown in the upper-right panel of Figures 7 and 8, is composed by two infinite tongues spiraling around the stable manifold to the third quadrant periodic orbit. The
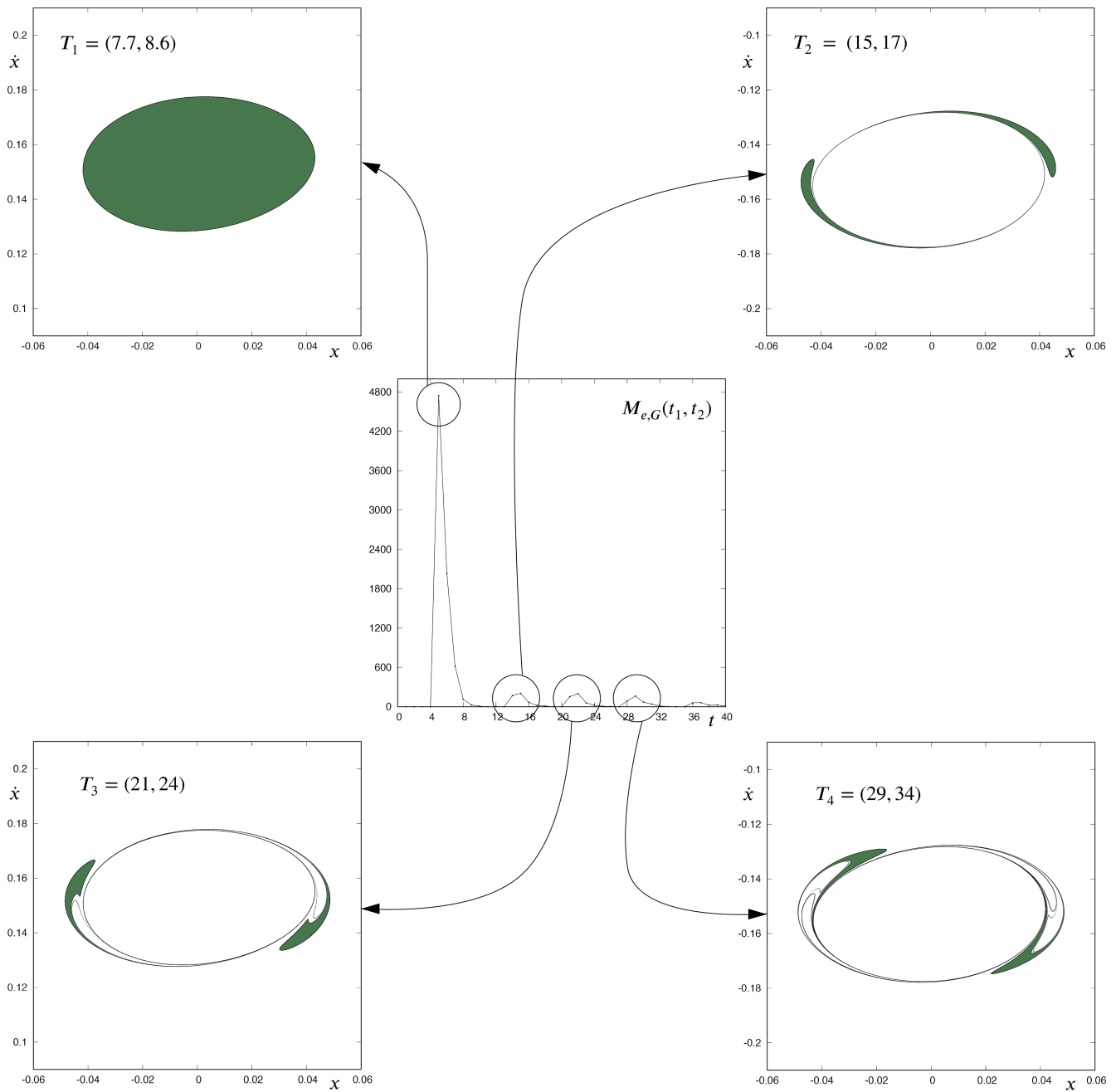
FIGURE 9 Origin of each of the hills depicted in Figure 6. The number of orbits that escape in each of the hills is related to the area occupied by the green colored region in each intersection of the stable manifolds to the Lyapunov orbits with the surface of section [Colour figure can be viewed at wileyonlinelibrary.com]

origin of these tongues is described in detail by Navarro,[7] and the region delimited by them tongues is colored in green. Each of the initial conditions belonging to this region correspond to orbits that exit the galaxy after intersecting the surface of section at one instant of time. The times of the second intersection belong to the interval $T_2 = (15,17)$. The structure of the third and fourth intersection of the stable manifold to ϕ becomes more complex and its composition is explained in detail by Navarro.[7] Their intersection times belong to the intervals $T_3 = (21,24)$ and $T_4 = (29,34)$, respectively.

Therefore, we can conclude that the origin of the sequence of hills we observe in the right panel of Figure 6 can be found in the distribution of the times of intersection of the stable manifolds to the Lyapunov orbits located at each of the openings of the potential well with the surface of section. Thus, the initial conditions colored in green in the upper-left panel of Figures 7 and 8 leave the potential with a time of escape in the interval $(4, 8)$, that is, with times slightly smaller than those of T_1. The same happens with the rest of the intersections.

Figure 9 tries to clarify the origin of each of the hills depicted in Figure 6. The number of orbits that escape in each of the hills are related to the area occupied by the green colored region in each intersection of the stable manifolds to the Lyapunov orbits with the surface of section.

4 | CONCLUSIONS

In this paper, we have started a numerical exploration of the escape in two systems with the same number of exit channels in the curves of zero velocity. To this purpose, we have integrated a mesh of 512×512 equally spaced initial conditions in the surface of section defined by $y = 0$, $\dot{y} = 0$, in both problems, determining, for each initial condition, if the corresponding orbit escapes from the system or remains trapped "forever." The results we have obtained unveil that the number of escaping orbits tends to zero as the time of escape becomes larger, despite of the fact that the way the escape occurs for relative small times of escape is significantly different between one system and the other. In the four-body ring problem, the distribution of the number of escaping orbits is approximately uniform and slowly decreasing with time, for times of escape from 0 to 40, and considering intervals of time of unit size. However, in the galactic system, the fast escape of a particle from the system takes place sequentially, step by step. This different behavior is due to the way the stable manifolds are projected on the surfaces of section in both systems. In some sense, we can state that these projections have an orderer structure in the galactic system.

One could ask if the use of a surface of section avoiding the Lyapunov orbits in the four-body ring problem could alter the numerical results from a qualitative point of view, or if the variation of β affects the escape and if there is any value of this parameter for which we could find a similar behavior of the escape in both systems. These and some other open questions will guide our future work.

CONFLICT OF INTEREST

The authors declare no potential conflict of interest.

ORCID

Juan F. Navarro https://orcid.org/0000-0002-5898-2786

REFERENCES

1. Aguirre J, Sanjuan MAF. Limit of small exits in open Hamiltonian systems. *Phys Rev E*. 2003;67:056201.
2. Barbanis B. Escape regions of a quartic potential. *Celest Mech Dyn Astron*. 1990;48(1):57-77.
3. Barrio R, Blesa F, Serrano S. Bifurcations and safe regions in open Hamiltonians. *New J Phys*. 2009;11:053004.
4. Contopoulos G. Asymptotic curves and escapes in Hamiltonian systems. *Astron Astrophys*. 1990;231(1):41-45.
5. Contopoulos G, Kaufmann D. Types of escapes in a simple Hamiltonian system. *Astron Astrophys*. 1992;253(2):379-388.
6. Navarro JF, Henrard J. Spiral windows for escaping stars. *Astron Astrophys*. 2001;369:1112-1121.
7. Navarro JF. Windows for escaping particles in quartic galactic potentials. *Appl Math Comput*. 2017;303:190-202.
8. Navarro JF. On the escape from potentials with two exit channels. *Sci Rep*. 2019;9:13174.
9. Navarro JF. On the integration of an axially symmetric galaxy model. *Comp Math Methods*. 2019;1(1–14).
10. Navarro JF. Limiting curves in an axially symmetric galaxy. *Math Meth Appl Sci*. 2021;44:993-1002.
11. Navarro JF. Dependence of the escape from an axially symmetric galaxy on the energy. *Sci Rep*. 2021;11:8427.
12. Navarro JF. A proper surface of section to study a new Hénon–Heiles potential with additional singular gravitational terms. *Eur Phys J Plus*. 2021;136:537.

13. Navarro JF, Martinez–Belda MC. On the use of surfaces of section in the *N*-body problem. *Math Meth Appl Sci.* 2020;43:2289-2300.

14. Navarro JF, Martinez–Belda MC. Escaping orbits in the *N*-body ring problem. *Comp Math Methods.* 2020;2:1-14.

15. Navarro JF, Martinez–Belda MC. On the analysis of the fractal basins of escape in the *N*-body ring problem. *Comp Math Methods.* 2020:e1131.

16. Navarro JF, Martinez–Belda MC. Analysis of the distribution of times of escape in the *N*-body ring problem. *J Comput Appl Math.* 2021:113396.

17. Siopsis C, Kandrup HE, Contopoulos G, Dvorak R. Universal properties of escape in dynamical systems. *Celest Mech Dyn Astron.* 1996;65(1–2):57-68.

18. Zotos EE. Trapped and escaping orbits in an axially symmetric galactic-type potential. *PASA.* 2012;29:161-173.

19. Zotos EE, Cheng W, Navarro JF, Saeed T. A new formulation of the Hénon–Heiles potential with additional singular gravitational terms. *Int J Bifurcation Chaos.* 2020;30(13):2050197.

20. Navarro JF. Numerical integration of the *N*-body ring problem by recurrent power series. *Celest Mech Dyn Astr.* 2018;30:16.

21. Deprit A, Henrard J. Construction of orbits asymptotic to a periodic orbit. *Astron J.* 1969;74:308-316.